Bulgarian Chemical Communications, Volume 50, Special Issue J (pp. 156–164) 2018

Syntheses and vibrational spectroscopic characteristics of series ionic merocyanine dyes

M. Todorova[1], R. Bakalska[2]*

[1] *University of Food Technology, Faculty of Technology, Department Organic Chemistry, 26 Maritsa Blvd., 4000 Plovdiv, Bulgaria*
[2] *Plovdiv University, Faculty of Chemistry, Department Organic Chemistry, 24 Tzar Assen Str., 4000 Plovdiv, Bulgaria*

Received March, 2018; Revised April, 2018

A series ionic merocyanine dyes with enlarged π-conjugated system and varying length of the N-alkyl chain were synthesized and investigated by means of solid-state IR and Raman spectroscopy. Quantum chemical calculations at the DFT level were performed to predict electronic structure and vibrational data. Nearly all IR bands are asymmetric. As a result of electronic interaction due to the intramolecular charge transfer (ICT) which leads to vibrational one, nearly all vibrations are strongly mixed and the intensities are strong influenced. For this reason, the vibrational spectroscopy does not help to estimate the contribution of the two final forms – benzenoid and quinoid in the real electronic structure of the dyes. IR and Raman data for the various dyes are with close numerical values to that of the predicted ones.

Keywords: Merocyanine dye; Styrylquinolinium dye; IR and Raman spectroscopy; DFT calculations.

INTRODUCTION

Merocyanines are systems exhibiting the intramolecular charge transfer (ICT) between the electron-donating and -withdrawing end groups along the conjugated bonds in the polymethine chain, which in terms of the classical resonance theory is described by a linear combination of limiting resonance structures – benzenoid and quinoid, as shown in Scheme 1. Due to their strongly pronounced solvatochromism and the abilities to change their dipole moment essentially at electronic excitation as well as to sensitize various physical and chemical processes, merocyanines find wide application in optoelectronics, nonlinear optics, devices for information recording, in medicine and biology [1–13].

The main method for investigation of the dyes and especially intramolecular charge transfer complex is the electron spectroscopy. NMR spectroscopy has also been used [14], but all these studies were carried out in solutions, and the electronic states of dyes could substantially vary depending on the solvent used. In the crystal, the ICT in merocyanines can be proved by the bond length alternation (BLA) parameter based on the X-ray diffraction study. Vibrational spectroscopy is usually the only method of structural elucidation of dyes in solid state [15]. Kolev and co-workers have successfully applied the X-ray diffraction and vibrational spectroscopy for structural elucidation of dyes in solid state to prove the hyperpolarizabilities of a number of dye chromophores [16–21].

The goal of the present study was to reveal the distinguishing features of the vibrational spectra of merocyanines and to establish general relations between vibrational spectra and their electronic asymmetry determined by donor-acceptor power of the terminal fragments. Therefor we synthesized a series of styrylquinolinium dyes **5**–**8** with enlarged π-conjugated system, belonging to the merocyanine class. The accent is on the study of the dyes by IR and Raman spectroscopy. Quantum chemical DFT calculations at the B3LYP level of theory using a 6-311++G** basis set were applied for predicting the structure and vibrational data of the chromophore (**5**).

EXPERIMENTAL

The synthesis of dye (**5**) has been reported in the literature [22]. All dyes studied were obtained

* To whom all correspondence should be sent:
E-mail: bakalska@uni-plovdiv.net

according to modified by us procedure of higher yields similar to that already outlined for dye (**6**) in our earlier work [12]. The preparation of 1-alkyl-4-methylquinolinium halogenides (**1**–**4**) was described in Ref. [23].

*General method for preparation of hydroxy-substituted dyes (**5**–**8**)*

A mixture of 1-alkyl-4-methylquinolinium halogenides (1.25 mmol), 4-hydroxynaphtaldehyde (1.25 mmol), piperidine (0.25 mmol) and glacial acetic acid (0.25 mmol) in dry benzene (20 mL) was heated under reflux, equipped with Dean-Stark apparatus and drying tube. After boilling during 6 h, the reaction mixture was cooled; the solid was filtered off, washed with benzene and dried at room temperature. All derived dyes were recrystallized from methanol. Yields 85–95%. All of these salts were characterized by ^{1}H and ^{13}C NMR, UV-Vis and fluorescence, mass spectroscopy and thermal methods [23].

Vibrational and computational methods

The solid state IR and Raman spectra were recorded between 4000 cm^{-1} and 400 cm^{-1} on a VERTEX 70 FT-spectrometer (Bruker Optics). 50 scans were performed for each spectrum with a resolution of 2 cm^{-1}. All density functional theory (DFT) computations were performed with the GAUSSIAN 03 program package [24] employing the B3LYP (Becke's three-parameter non-local exchange) [25, 26] correlation functional and 6-311++G** basis set.

RESULTS AND DISCUSSION

Syntheses

The synthesis of styrylquinolinium dyes (**5**–**8**) was carried out by Knoevenagel condensation of N-alkyl lepidinium halogenide (**1**–**4**) and 4-hydroxynaphtaldehyde in the presence of catalyst piperidine/ glacial acetic acid. The synthesis is depicted in Scheme 1. The real dye structure can be represented by a set of the limiting resonance structures – benzenoid and quinoid. Four p-hydroxy substituted dyes with varying the length of the alkyl chain of C1 to C4, namely: 4-[(*E*)-2-(4-hydroxynaphthalen-1-yl) ethenyl]-1-methylquinolinium iodide (**5**); 4-[(*E*)-2-(4-hydroxynaphthalen-1-yl)ethenyl]-1-ethylquinolinium bromide (**6**); 4-[(*E*)-2-(4-hydroxynaphthalen-1-yl)ethenyl]-1-propylquinolinium iodide (**7**); 4-[(*E*)-2-(4-hydroxynaphthalen-1-yl)ethenyl]-1-butylquinolinium bromide (**8**) were investigated.

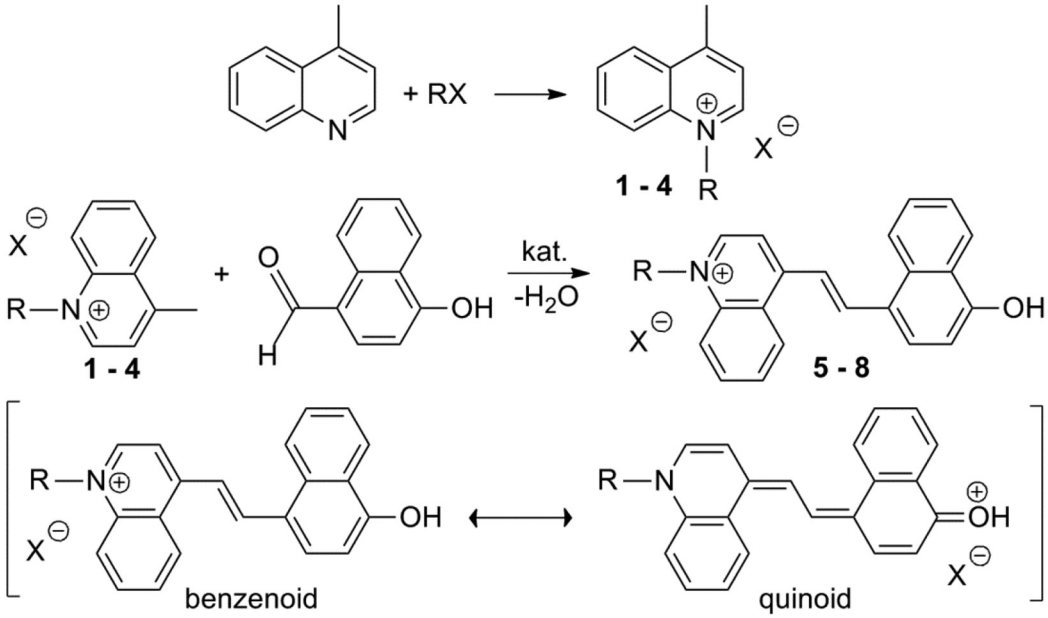

1: R = Me, X = I
2: R = Et, X = Br
3: R = n Pr, X = I
4: R = n Bu, X = Br
5: R = Me, X = I
6: R = Et, X = Br
7: R = n Pr, X = I
8: R = n Bu, X = Br

Scheme 1. Reaction scheme for obtaining of merocyanine dyes (**5**)–(**8**) presented with the limiting resonance structures – benzenoid and quinoid.

Vibrational and computational analysis

The accurate assignment of the main experimental frequencies of compounds (**5**)–(**8**) to the corresponding normal modes was supported by B3LYP/6-311++G** calculations. The IR spectra of the series of 4-hydroxy dyes with the same chromophore and different long N-alkyl chain were shown on Figure 1 and in the Table 1 are summarized selected experimental and calculated vibrations. In some cases where more than one band were observed we assigned the band which is closest by frequency to the predicted band by the theoretical method. That phenomenon could be explained with availability of crystal effects [15].

It should be noted that in general the spectral picture in IR spectra is complicated and needs very detailed regard. Nearly all IR bands are asymmetric. Since, the electron interaction between a strong donor – phenolic hydroxyl group and the strongest acceptor – quinolinium fragment leads to vibrational interaction, as a result of this nearly all vibrations are strongly mixed and the intensities are strong influenced. The so-called Davydov splitting and Evans holes effects were observed in all spectra and these phenomenona could be explained with availability of crystal field effects [15]. There is also a characteristic elevation of the spectrum background typical for the salts in the solid state.

In the IR spectra of the merocyanine dyes under study, the stretching vibration of phenolic OH group was found as a broad band in the range 3429–3344 cm^{-1} (Fig. 1). This indicates that a hydrogen bond exists. Only in the IR spectrum of the dye **5** two bands for the stretching vibration of the OH group at 3429 cm^{-1} and 3391 cm^{-1} were detected, caused by the solid state effects. The stretching vibration bands of the OH group are downshifted of 200 to 400 cm^{-1} in comparison to theoretic ones. The maxima at 2963 cm^{-1} and 2875 cm^{-1} correspond to asymmetric and symmetric C–H stretching vibrations of the methyl group, while these ones in the range 2980–2920 cm^{-1} of the symmetrical and asymmetrical C–H stretching vibrations of methylene group/s.

The bands at about 1618 and 1609 cm^{-1} belong to the skeletal vibration ν(C=C) of the naphthalene fragment resembling the oscillation 8a. The most intense bands in the infrared spectra of the dyes at about 1588 and 1560 cm^{-1} refer to the highly mixed $\nu_{C=C}$ and 8a, 8b plane vibrations of the quinoline fragment of the molecules and this one at 1575 cm^{-1} to mixed vibration ν(C=C) of the naphthalene, ν(C=C) of the quinoline nucleus and deformation vibration of methyl group. To the in-plane deformation mode β(C–H) of the naphthalene fragment correspond two maxima at about 1473 cm^{-1} and 1441 cm^{-1}, respectively. Some bands at about 1351, 1340, 1270 and 1235 cm^{-1} for the β(C–H) vibrations of the quinoline part were also observed (Table 1). The maximum corresponding to the C–H deformation vibrations of the methyl group is found at about 1142 cm^{-1}, and those of the out-of-plane γ(C–H) of the aromatic rings at about 1004–1014 cm^{-1}. To antiphase vibration γ(C–H) of the quinoline fragment corresponds the band at about 970 cm^{-1}.

In the Raman spectra the asymmetric bands are not so much opposed to the IR spectra but both allows better assignment of the bands. For strongly polar chemical bonds such as O–H, C–H, etc., the bands are of low intensity. This explains why in the Raman spectra of the compounds there are miss-

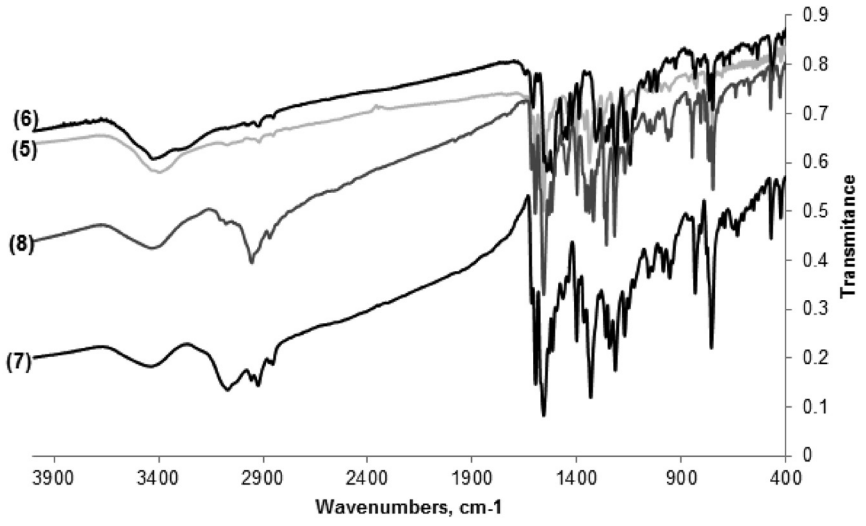

Fig. 1. Solid-state IR-spectra of merocyanine dyes (**5**)–(**8**) in the region of 4000–400 cm^{-1}.

Table 1. Theoretically predicted frequencies, the measured IR and the assignment of the bands to the corresponding normal vibrations of the dyes (**5**)–(**8**)

Vibrational Assignments	Calc. IR Frequency [cm^{-1}]	Observed IR Frequency [cm^{-1}]			
		(5)	**(6)**	**(7)**	**(8)**
ν (OH), pure	3813	3426 3391 br	3426 3290 sh	3429 br	3429 br
ν^{s} (CH_3), pure	3057	3056	3067	3067	3067
ν^{as} (CH_2) + ν^{s} (CH_2)	2978	–	2974	–	–
ν^{as} (CH_3) +ν^{as} (CH_2) + ν^{s} (CH_2)	2958	–	–	2960	2954
ν^{s} (CH_3) ν^{as} (CH_2) + ν^{s} (CH_2)	2929	–	2923	2920	2924 sh
ν (C=C) NF (8a) + ν(C=C)	1627	1622	–	–	–
ν(C=C) NF (8a)	1611	1614	1609	1614	1618
ν(C=C) + ν(C=C) NF + ν(C=C)QF (8b)	1588	1586	1586	1591	1592
ν(C=C) QF + ν(C=C) NF + δ (CH_3)	1575	1575sh	–	1572 sh	1575 sh
ν(C=C)NF(19a) + ν(C=C) QF	1556	1558	1556	1556	1557
δ^{s} (CH_3) QF + ν(C=C) QF	1519	1520	1518 sh	1514	1518
ν(C=C) NF (19a)	1502	1506	1507	–	–
δ^{as} (CH_3)	1489	1486	1488	–	–
β(C-H) NF	1473	1473	1471	1465	1470
δ^{s}(CH_3)+ β(C-H) QF	1459	1467	1458	1458 sh	1454 sh
β(C-H) NF	1441	1439	1445	1439	1447
β(C-H) NF + δ^{s} (CH_3) + ν(N-C) QF	1425	1421	1423	–	–
β(C-H) C=C + ν(C=C) NF + ν(C-H) QF + δ^{s} (CH_3)	1406	1400	–	1400	1398
βC-H (C=C) + ν (C-O) NF	1381	1388	1390	1383	-
ν(N-C) QF + δ(C=C) QF + βC-H (C=C) + δ(CH_3)	1377	1375	1377 sh	–	1372 sh
β(C-H) NF + β(C-H) QF + ν(C=C) NF + ν(C=C) QF	1361	1361	–	1365	1356
βC-H (C=C) + β(C-H) NF + β(C-H) QF	1351	1353	1356	–	–
βC-H (C=C) + β(C-H) NF + β(C-H) QF	1334	1338	1343	1343 sh	1339
β(C-H) NF (3)+ βC-H (C=C)	1328	1330	1331	1333	1319
β(C-H) QF + βC-H (C=C) + ν(C-N)	1302	1310	1307	1313	1307
βC-H (C=C) + δ(O-H)	1283	1284	1298	1290	1293
β(C-H) NF + β(C-H) QF	1271	1271	1266	–	1268
ν(C-N) QF+ β(C-H) QF	1254	1249	1249	1259	1258
βC-H (C=C) + δ (O-H) + β(C-H) QF	1235	1236	–	–	–
β(C-H) NF + β(C-H) QF + δ (O-H)	1220	1224	1222	1217	1219
β(C-H) QF + δ(CH_3) + β(C-H) NF	1217	1211	1208	1215	–
β(C-H) NF + δ(CH_3)	1199	1199	–	–	–
β(C-H) NF + β(O-H)	1170	1167	1169	1172	1170
δ (CH_3)	1140	1142	1145	1150	1152
δ(CH_3) + ν(C-N)	1128	1132	1121	1124	1131
β(C-H) NF + β(O-H) + βC-H (C=C)	1082	1083	–	1088 sh	–
β(C-H) QF + βC-H (C=C)	1067	1070	–	–	1073 sh
β(C-H) NF + βC-H (C=C)	1064	–	–	1055	1063
breathing NF + βC-H (C=C)	1036	1037	1039	1036	1045
β(C-H) QF + β(C-H) NF + βC-H (C=C)	1031	1032	–	–	1031
γ(C-H) QF	1019	1018	1019	–	–

Table 1. (continued)

γ(C-H) NF	1012	1014	–	1005	1004
γ(C-H) QF + γC-H (C=C)	997	997	998	987	994
antiphase γ(C-H) QF, pure	970	971	963	–	972
antiphase γ(C-H) NF	953	953	951	955	955
βC-H (C=C) + γC-H (C=C)	898	899	901	–	900
β(C-H) NF + β(C-H) QF	876	875	875	–	870
β(C=C)NF + β(C=C) + β(C=C)QF	850	846	852	–	848
γ(C-H) NF + γ(C-H) QF + δ(C=C)NF	827	830	833	833	825
β(C=C) QF	814	811	809	–	–
δ(C=C) NF, δ(C=C) QF + β(C=C)	801	798	–	806	807
δ(C=C) NF + γ(C-H) NF + γ(C-H)QF	784	–	–	–	785
"umbrella mode" NF + "umbrella mode" QF	780	782	781	–	–
β(C-H) NF + δ(C-N) QF	776	763	767	758	770
β (C=C) QF + β (C=C) NF	712	697	707	709	706
ring puckering QF (4) + NF	666	668	669	–	665
ring puckering NF + QF	654	648	659	654	648
skel. def. QF + NF	627	624	624	633	636
ring puckering γ(C=C)NF + γ(C=C)QF, "umbrella mode" NF	611	–	608	605	601
γC-H $_{(C=C)}$ + β(C=C) QF + γ(C=C)NF	583	588	586	588	–
γ (C=C) QF + β (C=C) NF + γ(O-H)	564	569	569	577	574
β(C=C) QF + β(C=C)NF	556	559	559	555	556
β(C=C) QF + β(C=C) NF	507	–	512	507	505
β(C=C) NF + γ(C=C) QF	500	501	501	–	500
β(C=C) NF + β(C=C) QF	485	490	–	490	485
ring puckering NF (4) + QF	478	471	–	471	471
skel. def. NF + β(C=C) QF	466	461	460	–	464
ring puckering NF + γ(O-H)	431	426	428	–	426

Abbreviations: QF (quinolinium fragment), NF (naphthalene fragment); ν – stretching, δ – deformation, β – in-plane deformation, γ – out-of-plane, τ – torsion vibrations; br. – broad, sh. –shoulder.
Scaling factor –0.9688 [27]

ing bands for O–H and C–H vibrations and why in Fig. 2 the shown region of the Raman spectrum of dye (**8**) is in the range 1800–400 cm^{-1}. The predicted frequencies, selected measured Raman ones and the assignment of the bands to the corresponding normal vibrations were listed in Table 2. The dye (**7**) Raman frequencies were not included in Table 2 because it exhibits a tendency to photodegradation even at the lowest power of the laser source.

As already mentioned, the vibrational spectra are strongly deformed from the charge transfer complex (CT), and it is an evidence of its existence proven by the vibration spectroscopy method. Unfortunately, the vibrational spectroscopy is not enough to quantify the real electronic structure of the molecules according to the contribution of the two forms – benzenoid and quinoid. The reason is that the vibrations of $\nu_{C=O}$ and $\nu_{C=C}$ are mixed and with close numerical values. It is noteworthy, that the data from the experimental IR and Raman spectra for the various dyes are of close numerical values and within the error. The probable explanation is that for the same chromophore, the influence of the N-alkyl group on the ICT is negligible (weak +I effect). This explanation is also required by the UV-Vis spectra of dyes **5**–**8**, shown on Fig. 3, all measured in methanol, whose maxima are very close. The shorter-wave absorption bands at 493±2 nm were referred to the CT-band of the benzenoid structures of the dyes, and the longer wavelength bands – to the quinoid forms (Fig. 3, Scheme 1). The longer wavelength band splits into two bands

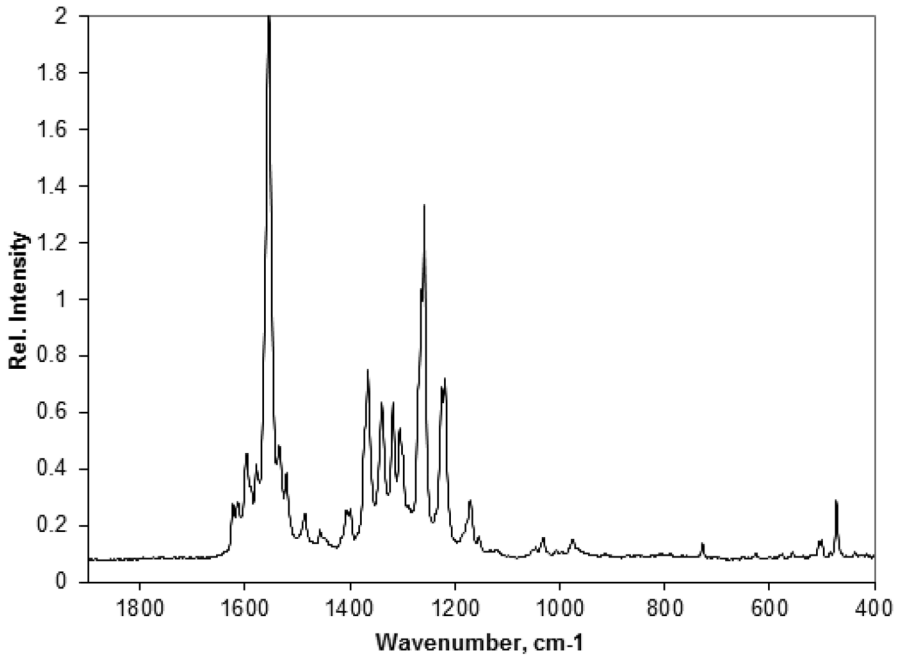

Fig. 2. Raman spectrum of the dye (**8**) in the region of 1800–400 cm^{-1}.

Table 2. Theoretically predicted frequencies, selected experimental Raman frequencies and the assignment of the bands to the corresponding normal vibrations of the dyes (**5**), (**6**) and (**8**)

Vibrational Assignments	Calc. Raman Frequency [cm^{-1}]	Observed Raman Frequency [cm^{-1}]		
		(5)	**(6)**	**(8)**
ν (C=C) NF (8a) + ν(C=C)	1627	1623	1626	1624
ν(C=C) NF (8a)	1611	1608	1616	1615
ν(C=C) + ν(C=C) NF + ν (C=C) QF (8b)	1588	1590	1595	1595
ν(C=C) QF+ ν(C=C) NF + δ(CH_3)	1575	1578	1579	–
ν(C=C) NF (19a) + ν(C=C) QF	1556	1552	1552	1555
δ^s (CH_3) QF + ν(C=C) QF	1519	1520	–	1522
ν(C=C) QF + δ(CH_3) (19a)	1491	1492	–	1484
δ^s(CH_3)+ β(C-H) QF	1459	1459	–	1458
β(C-H) C=C +ν(C=C) NF +ν(C-H) QF + δ^s (CH_3)	1406	1402	1397	1408
ν(N-C) QF + δ(C=C) QF+ βC-H (C=C) + δ(CH_3)	1377	1375	1372	–
β(C-H) NF + β(C-H) QF + ν(C=C) NF + ν(C=C) QF	1361	1365	1363	1366
βC-H (C=C) + β(C-H) NF + β(C-H) QF	1334	1343	1336	1340
β(C-H) NF (3)+ βC-H (C=C)	1328	1327	1332	1319
β(C-H) QF + βC-H (C=C) + ν(C-N)	1302	1310	1306	1304
βC-H (C=C) + δ(O-H)	1283	1292	1286	–
β(C-H) NF+ β(C-H) QF	1271	1275	1270	1269
ν(C-N) QF+ β(C-H) QF	1254	1253	–	1258
β(C-H) NF + β(C-H) QF +δ (O-H)	1220	1224	1222	1220
β(C-H) QF + δ(CH_3) + β(C-H) NF	1217	1214	1217	1218
β(C-H) NF + δ(CH_3)	1199	1198	1194	–
β(C-H) NF + β(O-H)	1170	1169	1168	1169

Table 2. (continued)

δ (CH_3)	1140	1147	1146	1149
δ(CH_3) + ν(C-N)	1128	1128	1120	–
β(C-H) NF + β(O-H) + βC-H (C=C)	1082	1088	1090	–
β(C-H) NF + βC-H (C=C)	1064	1059	1069	–
breathing NF + βC-H (C=C)	1036	1036	1044	1045
β(C-H) QF + β(C-H) NF + βC-H (C=C)	1031	1032	–	1029
γ(C-H) QF	1019	1018	1017	–
γ(C-H) NF	1012	1012	1007	–
γ(C-H) QF + γC-H (C=C)	997	995	998	–
antiphaseγ(C-H) QF, pure	970	–	973	978
antiphase γ(C-H) NF	953	945	953	–
β (C=C) QF + β (C=C) NF	712	714	705	719
skel. def. QF + NF	627	629	–	629
Ring puckering γ(C=C) NF + γ(C=C) QF "umbrella mode" NF	611	608	602	–
γ(C=C) QF + β(C=C) NF + γ(O-H)	564	561 sh	573	–
β(C=C) QF + β(C=C)NF	556	556	–	557
β(C=C) QF + β(C=C) NF	549	542	540	–
β(C=C) QF + β(C=C) NF	507	506	–	504
β(C=C) NF + γ(C=C) QF	500	501	499	502
ring puckering NF (4) + QF	478	477	479	472
skel. def. NF + β(C=C) QF	466	465	465	–

Abbreviations: see footnotes under Table 1.

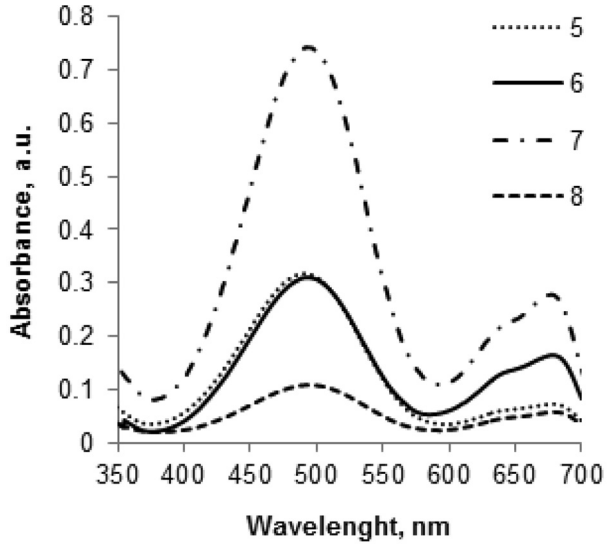

Fig. 3. UV-Vis spectra of merocyanine dyes (**5**)–(**8**) recorded in methanol.

with λ_{max} at 680 nm and 640 nm, demonstrating the aggregation phenomenon.

CONCLUSIONS

The coincidence between the calculated and measured frequencies is good and the complete vibrational analysis can be used for the calculation of the vibrational hyperpolarizability of the dyes.

Acknowledgments: *The authors thank Scientific Research Fund of the University of Plovdiv (project No FP17-HF-013), for financial support.*

REFERENCES

1. C. Bosshard, M. Bösch, I. Liakatas, M. Jäger, P. Günter, Nonlinear optical effects and materials, Springer-Verlag, Berlin, 2000.

2. H. S. Nalwa, T. Watanabe, S. Miyata, Nonlinear optics of organic molecules and polymers, CRC Press, Boca Raton, Florida, 1997.
3. L. R. Dalton, P. A. Sullivan, D. H. Bale, *Chem. Rev.*, **110**, 25 (2010).
4. P. Gregory, Industrial Dyes: Chemistry, Properties, Applications, Wiley-VCH, Weinheim, 2003.
5. S.-H. Kim, Functional Dyes, Elsevier, Amsterdam, 2006.
6. T. Kolev, I. V. Kityk, J. Ebothe, B. Sahraoui, *Chem. Phys. Lett*., **443**, 309 (2007).
7. T. Kolev, B. B. Koleva, M. Spiteller, H. Mayer-Figge, W. S. Sheldrick, *Dyes Pigm.*, **79**, 7 (2008).
8. B. B. Koleva, T. Kolev, R. Nikolova, Y. Zagraniarsky, M. Spiteller, *Cent. Eur. J. Chem.*, **6**, 592 (2008).
9. T. Kolev, B. Koleva, J. Kasperczyk, I. Kityk, S. Tkaczyk, M. Spiteler, A. H. Reshak, W. Kuznik, *J. Mater. Sci.: Mater. Electron*., **20**, 1073 (2008).
10. B. Koleva, S. Stoyanov, T. Kolev, I. Petkov, M. Spiteller, *Spectrochim. Acta, Part A*, **71**, 1857 (2009).
11. A. V. Kulinich, A. A. Ishchenko, *Russ. Chem. Rev.*, **78**, 141 (2009).
12. H. E. Ouazzani, S. Dabos–Seignon, D. Gindre, K. Iliopoulos, M. Todorova, R. Bakalska, P. Penchev, S. Sotirov, T. Kolev, V. Serbezov, A. Arbaoui, M. Bakasse, B. Sahraoui, *J. Phys. Chem. C*, **116**, 7144 (2012).
13. Y. Hubenova, R. Bakalska, E. Hubenova, M. Mitov, *Bioelectrochemistry*, **112**, 158 (2016).
14. A. V. Kulinich, A. A. Ishchenko, U. M. Groth, *Spectrochim. Acta, Part A*, **68**, 6 (2007).
15. B. Ivanova, T. Kolev, CRC Press, Taylor & Francis Group, Boca Raton, London, New York, 2012.
16. T. Kolev, B. B. Koleva, S. Stoyanov, M. Spiteller, I. Petkov, *Spectrochim. Acta, Part A*, **71**, 1857 (2009).
17. S. Stoyanov, B. B. Koleva, T. Kolev, I. Petkov, M. Spiteller, *Pol. J. Chem.*, **82**, 2167 (2008).
18. T. Kolev, T. Tsanev, S. Kotov, H. Mayer-Figge, M. Spiteller, W. S. Sheldrick, B. Koleva, *Dyes Pigm.*, **82**, 95 (2009).
19. B. B. Koleva, T. Kolev, M. Lamshoeft, M. Spiteller, W. Sheldrick, *Spectrochim. Acta A*, **74**, 1120 (2009).
20. R. Bakalska, M. Todorova, H. Sbirkova, B. Shivachev, T. Kolev, *Dyes Pigm.*, **136**, 919 (2017).
21. M. Todorova, R. Bakalska, T. Kolev, *Spectrochim. Acta A*, **108**, 211 (2013).
22. S. Hunig, O. Rosenthal, *Justus Liebigs Ann. Chem.*, **592**, 161 (1955).
23. M. Todorova, PhD Thesis, Plovdiv University, Plovdiv, 2015.
24. M. J. Frisch, G. W. Trucks, H. B. Schlegel, G. E. Scuseria, M. A. Robb, J. R. Cheeseman, G. Scalmani, V. Barone, B. Mennucci, G. A. Petersson, H. Nakatsuji, M. Caricato, X. Li, H. P. Hratchian, A. F. Izmaylov, J. Bloino, G. Zheng, J. L. Sonnenberg, M. Hada, M. Ehara, K. Toyota, R. Fukuda, J. Hasegawa, M. Ishida, T. Nakajima, Y. Honda, O. Kitao, H. Nakai, T. Vreven, J. A. Montgomery, Jr., J. E. Peralta, F. Ogliaro, M. Bearpark, J. J. Heyd, E. Brothers, K. N. Kudin, V. N. Staroverov, R. Kobayashi, J. Normand, K. Raghavachari, A. Rendell, J. C. Burant, S. S. Iyengar, J. Tomasi, M. Cossi, N. Rega, J. M. Millam, M. Klene, J. E. Knox, J. B. Cross, V. Bakken, C. Adamo, J. Jaramillo, R. Gomperts, R. E. Stratmann, O. Yazyev, A. J. Austin, R. Cammi, C. Pomelli, J. W. Ochterski, R. L. Martin, K. Morokuma, V. G. Zakrzewski, G. A. Voth, P. Salvador, J. J. Dannenberg, S. Dapprich, A. D. Daniels, O. Farkas, J. B. Foresman, J. V. Ortiz, J. Cioslowski, and D. J. Fox, Gaussian 03, Gaussian Inc., Wallingford CT, 2003.
25. P. J. Stephens, F. J. Devlin, C. F. Chabalowski, M. J. Frisch, *J. Phys. Chem.*, **98**, 11623 (1994).
26. C. T. Lee, W. T. Yang, R. G. Parr, *Phys. Rev. B*, **37**, 785 (1988).
27. J. Merrick, D. Moran, L. Radom, *J Phys Chem A*, **111**, 11683 (2007).

СИНТЕЗ И ВИБРАЦИОННИ СПЕКТРОСКОПСКИ ХАРАКТЕРИСТИКИ НА СЕРИЯ ЙОННИ МЕРОЦИАНИНОВИ БАГРИЛА

М. Тодорова[1], Р. Бакалска[2]*

[1] *Университет по хранителни технологии, Технологичен факултет, Катедра Органична химия, бул. „Марица“ 26, 4000 Пловдив, България*
[2] *Пловдивски университет „П. Хилендарски“, Химически факултет, Катедра Органична химия, ул. „Цар Асен“ 24, 4000 Пловдив, България*

Постъпила март, 2018 г.; приета април, 2018 г.

(Резюме)

Серия йонни мероцианинови багрила с разширена π-спрегната система и различна дължина на N-алкилната верига бяха синтезирани и изследвани чрез твърдофазна ИЧ и раманова спектроскопия. За да се предскажат електронната структура и вибрационните характеристики, бяха извършени квантово-химични изчисления на ниво DFT. Почти всички инфрачервени ивици са асиметрични. В резултат на електронното взаимодействие, дължащо се на вътремолекулния пренос на заряд (ICT), което води до вибрационно взаимодействие, почти всички трептения са силно смесени, а интензитетите им са силно повлияни. Поради тази причина, вибрационната спектроскопия не дава възможност да се оцени приносът на двете крайни форми бензеноидна и хиноидна в реалната електронна структура на багрилата. Експерименталните и инфрачервени и раманови ивици за различните багрила са с близки числови стойности, както и с изчислените.